General relation between the group delay and dwell time in multicomponent electron systems

Feng Zhai and Junqiang Lu

Phys. Rev. B **94**, 165426 — Published 19 October 2016

DOI: 10.1103/PhysRevB.94.165426

General relation between the group delay and dwell time in multicomponent electron systems

Feng Zhai[1,2] and Junqiang Lu[2]
[1]*Department of Physics, Zhejiang Normal University, Jinhua 321004, China*
[2]*Department of Physics and Institute for Functional Nanomaterials, University of Puerto Rico, Mayaguez, PR 00681, USA*

For multicomponent electron scattering states, we derive a general relation between the Wigner group delay and the Bohmian dwell time. It is found that the definition of group delay should account for the phase of the spinor wave functions of propagating modes. The difference between the group delay and dwell time comes from both the interference delay and the decaying modes. For barrier tunneling of helical electrons on a surface of topological insulators, our calculations including the trigonal-warping term show that the decaying modes can contribute greatly to the group delay. The derived relation between the group delay and the dwell time is helpful to unify the two definitions of tunneling time in a quite general situation.

I. INTRODUCTION

For various quantum tunneling devices, the time scale of tunneling processes is a key parameter in performance evaluation. However, the lack of a time operator in quantum mechanics renders the definition of a physical tunneling time controversial[1–12]. Several time characteristics[4,5] have been introduced to describe different or complementary aspects of electron dynamics and can be extracted from corresponding optical or transport measurements[7]. Recently, the state-of-the-art ultrafast laser technology has been utilized to measure tunneling time delay during the strong field ionization of atoms[8–12]. This progress promises to clarify the applicability or physical regimes of different definitions of tunneling time.

The Wigner group delay and Bohmian dwell time, as two definitions of tunneling time, are considered well established[4]. The group delay (also called phase time) τ_g is expressed by the energy derivative of the scattering phase[2,6]. The dwell time τ_d represents the time spent by a particle following a Bohmian trajectory in the scattering region[3,12]. It concerns the entire wave function in the scattering region and does not distinguish transmission and reflection. Therefore τ_d was found to be related to the lifetime of corresponding resonant state[12]. For a one-dimensional (1D) barrier tunneling problem on scalar Schrödinger particles, Winful[6] has found that the group delay equals the dwell time plus a self-interference delay. The self-interference effect arises from the overlap of incident and reflected waves at the entrance of the scattering region. Recently, the Winful relation has been generalized to systems made of graphene monolayer[13–18] or bilayer[19]. It is commonly believed that for Dirac particles in graphene, the dwell time always equals the group delay[13–17,19]. However, in Ref. 18 it is shown that $\tau_d = \tau_g$ holds only for some special cases including Klein tunneling.

In this work, we explore the general relation between the dwell time and group delay for multicomponent electron scattering states. It is found that in multicomponent electron systems the group delay should be redefined to account for the uncertainty of scattering phase. The difference $\tau_g - \tau_d$ is contributed by both the interference delay and the evanescent modes. To illustrate the contribution of evanescent modes, we calculate the two tunneling times τ_g and τ_d for barrier tunneling of helical electrons on a surface of topological insulators where the trigonal-warping term is included.

II. MODEL AND FORMALISM

We begin with a 1D system schematically depicted in Fig. 1, which is described by the Hamiltonian (under the unit with $\hbar = 1$)

$$\hat{H} = \mathbf{A}_0 + \sum_{r=1}^{N} \mathbf{A}_r \hat{k}_x^r, \tag{1}$$

where $\hat{k}_x = -i\partial_x$ is the momentum along the transport direction, N is the highest order of momentum in the Hamiltonian, $\mathbf{A}_r$ (r = 0,1,...,N) is a $M \times M$ Hermitian matrix, and $\mathbf{A}_N$ is invertible. For simplicity, we assume that only $\mathbf{A}_0$ varies with the position x. Our results hold even for the general situation that all $\mathbf{A}_r$ ($0 \le r \le N$) are position-dependent. In the Landauer-Buttiker frame, transport problems in many systems ranging from nanowires with Majorana fermions[20,21] to electron waveguides with spin-orbit interaction[22] or topological edge states[23], can be reduced to solve the stationary Schrödinger equation $\hat{H}\Psi = E\Psi$. Here Ψ is an eigen wave function with energy E.

In the left lead ($x < 0$) where $\mathbf{A}_0(x) = \mathbf{A}_0(-\infty)$ is constant, the Hamiltonian has plane-wave-like solutions (called modes) $\Phi(x) = \psi \exp(ikx)$. The momentum k and related spinor ψ can be determined from an eigen problem (see Appendix A). For a propagating mode with real momentum k, the propagation direction is identified from its mean velocity

$$v_k = \frac{\partial E}{\partial k} = \frac{\Phi^\dagger \hat{v} \Phi}{\Phi^\dagger \Phi},\ \hat{v} = \frac{\partial \hat{H}}{\partial \hat{k}_x}. \tag{2}$$

Hereafter all propagating modes are normalized to have a unit velocity, i.e., $\Phi^\dagger \hat{v} \Phi = \pm 1$ or $\psi^\dagger \psi = 1/|v_k|$. We denote the set of left-decaying modes (with $\mathbf{Im}k < 0$) by LD and send the left-propagating modes (with $\mathbf{Im}k = 0$ and $v_k < 0$) to the set LP. For the incidence from a right-propagating mode $\Phi_{in}(x) = \psi_{in} \exp(ik_{in}x)$, the wave function in the left lead is written as

$$\Psi(x) = \Phi_{in}(x) + \sum_{j \in LP \cup LD} r_j \psi_j \exp(ik_j x), x < 0. \tag{3}$$

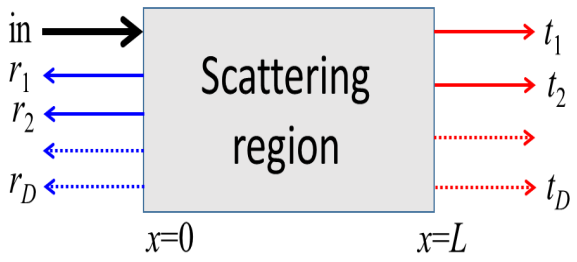

FIG. 1: (Color online) Schematic illustration of the considered system. The scattering region spans the region $0 < x < L$. The incident wave is depicted by the black thick solid arrow. The $D = MN/2$ reflected (transmitted) waves with amplitude r_1,r_2,...,r_D (t_1,t_2,...,t_D) are presented as blue (red) arrows. Solid/dotted arrows are for propagating/evanescent modes.

Here r_j is the reflection amplitude of the mode j.

In the right lead ($x > L$) with $\mathbf{A}_0(x) = \mathbf{A}_0(+\infty)$, one can also find NM modes where the right-decaying (right-propagating) modes comprise the set RD (RP). The scattering state Ψ in the right lead admits the form

$$\Psi(x) = \sum_{j\in RP\cup RD} t_j\psi_j \exp[ik_j(x-L)], x > L. \quad (4)$$

Here t_j is the transmission amplitude of the mode j. The conservation of probability current requires

$$T + R = 1, T = \sum_{j\in RP} |t_j|^2, R = \sum_{j\in LP} |r_j|^2, \quad (5)$$

where T and R are the transmission and reflection probability due to the incident wave Φ_{in}.

Under the normalization $\Phi_{in}^\dagger \hat{v}\Phi_{in} = 1$, the Bohmian dwell time in the scattering region ($0 < x < L$) is defined as[3,12]

$$\tau_d = \int_0^L \Psi^\dagger(x)\Psi(x)dx. \quad (6)$$

The Wigner group delay is given by the weighted sum of transmission and reflection group delays[4,6]

$$\begin{aligned}\tilde{\tau}_g &= \mathbf{Im}(\sum_{j\in LP} \bar{r}_j \frac{\partial r_j}{dE} + \sum_{j\in RP} \bar{t}_j \frac{\partial t_j}{dE}) \quad (7)\\ &= \sum_{j\in LP} |r_j|^2 \frac{\partial \arg r_j}{\partial E} + \sum_{j\in RP} |t_j|^2 \frac{\partial \arg t_j}{\partial E}.\end{aligned}$$

It should be noticed that this definition has a phase-related uncertainty. Firstly, the scattering state is unchanged when its wave function is multiplied by a global phase factor, i.e., $\Psi(x) \to \Psi(x)\exp(i\theta)$. Secondly, we can choose arbitrarily the phase of the spinor wave function of any mode, i.e., $\psi_j \to \psi_j \exp(-i\theta_j)$ for $j \in LP \cup RP$. Here θ and all θ_j depend smoothly on the energy E. To keep the scattering state unchanged after the two replacements, one has to do the transformation $r_j \to r_j \exp[(i(\theta_j + \theta)]$ for $j \in LP$ and $t_j \to t_j \exp[(i(\theta_j + \theta)]$ for $j \in RP$. It is evident that τ_g defined in Eq. (7) will change under this transformation. This is a reason for the discrepancy between Refs. 13–17 and Ref. 18. The definition of the group delay should be free of the artificial phase choice for either the scattering state or the spinor wave function of modes. We will show that the proper definition of group delay appears naturally in the expression of the dwell time.

A. Bilinear probability current density

To express τ_d in terms of the scattering amplitudes (r_j and t_j) and the lead information (k_j and ψ_j), it is useful to introduce a bilinear function related to the probability current density. For the Hamiltonian (1) and an eigenstate Ψ, the probability current density can be written as $J(\Psi, \Psi)$ where the bilinear function $J(\Psi_1, \Psi_2)$ reads

$$J(\Psi_1, \Psi_2) = \sum_{r=1}^{N}\sum_{s=0}^{r-1} (\hat{k}_x^s\Psi_1)^\dagger \mathbf{A}_r(\hat{k}_x^{r-1-s}\Psi_2). \quad (8)$$

Two properties of J (proved in Appendix B) will be utilized hereafter. One is that for any two states Ψ_1 and Ψ_2, we have

$$\Psi_1^\dagger(\hat{H}\Psi_2) - (\hat{H}\Psi_1)^\dagger\Psi_2 \equiv \hat{k}_x J(\Psi_1, \Psi_2). \quad (9)$$

In Appendix D, we show that even for a spatially-varying A_r ($0 \le r \le N$) there also exists a complicated bilinear function J satisfying Eq. (9).

Another useful property of J is that if $\Phi_1(x) = \exp(ik_1x)\psi_1$ and $\Phi_2(x) = \exp(ik_2x)\psi_2$ are two modes in a lead with energy E_1 and E_2 and satisfying $k_2 \neq \bar{k}_1$, then

$$J(\Phi_1, \Phi_2) = (E_2 - E_1)\frac{\exp[i(k_2 - \bar{k}_1)x]}{k_2 - \bar{k}_1}\psi_1^\dagger\psi_2. \quad (10)$$

Following Smith[3] and Winful[6], we differentiate $\hat{H}\Psi = E\Psi$ with respect to E and yield

$$\Psi^\dagger\Psi = \Psi^\dagger(\hat{H}\frac{\partial\Psi}{\partial E}) - (\hat{H}\Psi)^\dagger\frac{\partial\Psi}{\partial E} = -i\partial_x J(\Psi, \frac{\partial\Psi}{\partial E}).$$

Here we have used Eq. (9) with $\Psi_1 = \Psi$ and $\Psi_2 = \frac{\partial\Psi}{\partial E}$. This equation results in

$$\tau_d = i[J(\Psi, \frac{\partial\Psi}{\partial E})|_{x=0} - J(\Psi, \frac{\partial\Psi}{\partial E})|_{x=L}], \quad (11)$$

which relies on the wave function (3) and (4) in the left and right lead, but in a very complicated and implicit way.

B. Expression of the dwell time

To obtain the expression of τ_d, an alternative approach is to consider a scattering state Ψ_2 very close to Ψ. This state satisfies $\hat{H}\Psi_2 = (E + \Delta E)\Psi_2$. Its wave function in the left

and right lead is similar to Eqs. (3) and (4), but with the replacement $k_j \to k_j^{(2)}$, $\psi_j \to \psi_j^{(2)}$, $r_j \to r_j^{(2)}$, and $t_j \to t_j^{(2)}$. Here we assume that near the energy E the momentums k_j of all modes in a lead differ from each other and vary smoothly. This restriction can be relaxed if the lead has some conservation laws.

Using Eq. (9) with $\Psi_1 = \Psi$ and this Ψ_2 and integrating both sides over x, we arrive at

$$\int_0^L \Psi^\dagger \Psi_2 dx = \frac{i}{\Delta E}[J(\Psi,\Psi_2)|_{x=0} - J(\Psi,\Psi_2)|_{x=L}]. \quad (12)$$

In the limit of $\Delta E \to 0$, the left-hand side of Eq. (12) tends to τ_d. The right-hand side of Eq. (12) can be calculated straightforward with the help of Eq. (10). In its expression, the terms that diverge (converge) in the limit of $\Delta E \to 0$ are combined as iQ (iP), where P and Q are written as

$$\begin{aligned} P &= \sum_{j_1\neq j_2\in \mathbf{L}} \bar{r}_{j_1} r_{j_2}^{(2)} \frac{\psi_{j_1}^\dagger \psi_{j_2}^{(2)}}{k_{j_2}^{(2)} - \bar{k}_{j_1}} - \sum_{j_1\neq j_2\in \mathbf{R}} \bar{t}_{j_1} t_{j_2}^{(2)} \frac{\psi_{j_1}^\dagger \psi_{j_2}^{(2)}}{k_{j_2}^{(2)} - \bar{k}_{j_1}} \\ &+ \sum_{j\in LD} \bar{r}_j r_j^{(2)} \frac{\psi_j^\dagger \psi_j^{(2)}}{k_j^{(2)} - \bar{k}_j} - \sum_{j\in RD} \bar{t}_j t_j^{(2)} \frac{\psi_j^\dagger \psi_j^{(2)}}{k_j^{(2)} - \bar{k}_j} \\ &+ \sum_{j_1\in \mathbf{L}} [\bar{r}_{j_1} \frac{\psi_{j_1}^\dagger \psi_{in}^{(2)}}{k_{in}^{(2)} - \bar{k}_{j_1}} + r_{j_1}^{(2)} \frac{\psi_{in}^\dagger \psi_{j_1}^{(2)}}{k_{j_1}^{(2)} - k_{in}}], \end{aligned} \quad (13)$$

$$\begin{aligned} Q &= \sum_{j\in LP} \bar{r}_j r_j^{(2)} \frac{\psi_j^\dagger \psi_j^{(2)}}{k_j^{(2)} - k_j} + \frac{\psi_{in}^\dagger \psi_{in}^{(2)}}{k_{in}^{(2)} - k_{in}} \\ &- \sum_{j\in RP} \bar{t}_j t_j^{(2)} \frac{\psi_j^\dagger \psi_j^{(2)}}{k_j^{(2)} - k_j}. \end{aligned} \quad (14)$$

Here the set $\mathbf{L} = LD \cup LP$ and $\mathbf{R} = RD \cup RP$. If a general relation between the dwell time and the group delay exists, Q should be related to the group delay. The reason is that the group delay concerns the energy derivative of scattering phases which can appear only in $\lim_{\Delta E\to 0} Q$. The expression of Q up to $O(\Delta E)$ is derived in Appendix C, which is purely imaginary. The limit $\tau_g = -\lim_{\Delta E\to 0} \mathbf{Im} Q$ is then obtained,

$$\begin{aligned} \tau_g &= \mathbf{Im}[\sum_{j\in RP} \frac{\bar{t}_j \psi_j^\dagger (t_j\psi_j)'}{\psi_j^\dagger \psi_j} + \sum_{j\in LP} \frac{\bar{r}_j \psi_j^\dagger (r_j\psi_j)'}{\psi_j^\dagger \psi_j}] \\ &- \mathbf{Im}\frac{\psi_{in}^\dagger \psi_{in}'}{\psi_{in}^\dagger \psi_{in}}, \end{aligned} \quad (15)$$

where the prime indicates the derivative with respect to the energy E.

We define τ_g as the generalized group delay. In the case that the spinor parts ψ_j of all propagating modes have no energy dependence, τ_g reduces to Eq. (7). The difference between Eq. (7) and (15) comes from the presence of phase in the spinor wave function of propagating modes. Obviously, τ_g is independent of the phase choice for the spinor wave function of modes. Using Eq. (5), one can also check that the global phase change of the scattering state does not influence τ_g. This feature requires the occurrence of phase information of the incident wave [the last term in Eq. (15)].

Taking the limit on both sides of Eq. (12), we get the relation $\tau_d = \tau_g - \lim_{\Delta E\to 0} \mathbf{Im} P$, which together with Eq. (13) leads to

$$\tau_g = \tau_d + \tau_e + \tau_i, \quad (16)$$

$$\tau_e = \sum_{j\in RD} \frac{|t_j|^2 \psi_j^\dagger \psi_j}{2|\mathbf{Im} k_j|} + \sum_{j\in LD} \frac{|r_j|^2 \psi_j^\dagger \psi_j}{2|\mathbf{Im} k_j|}, \quad (17)$$

$$\begin{aligned} \tau_i &= \mathbf{Im}[\sum_{j\in \mathbf{L}} \frac{2 r_j \psi_{in}^\dagger \psi_j}{k_j - k_{in}} + \sum_{j_1\neq j_2\in \mathbf{L}} \frac{\bar{r}_{j_1} r_{j_2} \psi_{j_1}^\dagger \psi_{j_2}}{k_{j_2} - \bar{k}_{j_1}} \\ &- \sum_{j_1\neq j_2\in \mathbf{R}} \frac{\bar{t}_{j_1} t_{j_2} \psi_{j_1}^\dagger \psi_{j_2}}{k_{j_2} - \bar{k}_{j_1}}]. \end{aligned} \quad (18)$$

Equations (15)-(18) are the central results of this work. Due to the velocity normalization (and $\hbar = 1$), ψ_{in}, $r_j\psi_j$ and $t_j\psi_j$ in these equations have the same unit as $\sqrt{\partial k_{in}/\partial E}$. The difference between the generalized group delay τ_g and the dwell time τ_d equals the interference delay τ_i plus τ_e—the contribution only from evanescent waves. Note that τ_e is always nonnegative while τ_i can be negative. τ_i arises not only from the interference between the reflected waves and the incident wave (self-interference), but also from the interference among scattered waves. Evanescent waves can also contribute to τ_i. The presence of τ_e indicates that the escape of the entire wave function through the scattering region is not only via propagating modes but also by means of evanescent modes in leads. Note that although the scattering amplitude r_j and t_j depend on the phase choice of either the scattering state or the spinor wave function of propagating modes, the values of τ_e and τ_i in Eqs. (17) and (18) have no such a dependence.

C. Self-interference delay in graphene systems

In the systems[6,13–18] with $NM = 2$, the evanescent modes cannot coexist with propagating modes and thus $\tau_e = 0$. In these systems, the self-interference delay vanishes when perfect transmission occurs ($r_j = 0$). One such system is described by the 1D Schrödinger equation $[-\hat{k}_x^2/(2m) + V(x)]\Psi = E\Psi$ with mass m and scalar potential $V(x)$. For $\psi_j > 0$ the self-interference delay calculated directly from Eq. (18) is the same as in Ref. 6, i.e., $\tau_i = -\mathbf{Im} r/[2E - 2V(-\infty)]$.

Another such system is graphene-based devices where the leads are described by the massless Dirac Hamiltonian[13–18]

$$\hat{H}_{lead} = v_F(\sigma_x \hat{k}_x + \sigma_y \hat{k}_y).$$

Here $v_F > 0$ is the Fermi velocity, σ_x, σ_y together with σ_z are three Pauli matrices, and the transverse momentum $\hat{k}_y = -i\partial_y$ is conserved. We write the incident, reflected, and transmitted waves as the same in Ref. 13 (but with a unit

velocity)

$$\begin{aligned}\Psi_{in}(x) &= [1, se^{i\phi}]^T e^{ik_{in}x}/\sqrt{2v_{in}},\\ \Psi_{re}(x) &= r[1, -se^{-i\phi}]^T e^{-ik_{in}x}/\sqrt{2v_{in}},\\ \Psi_{tr}(x) &= t[1, se^{i\phi}]^T e^{ik_{in}(x-L)}/\sqrt{2v_{in}},\end{aligned} \tag{19}$$

where $s = \text{sign}(E)$, $k_{in} + ik_y = |E|\exp(i\phi)/v_F$, and $v_{in} = v_F\cos\phi$. The group delay is given by $\tau_g = \mathbf{Im}(\overline{r}r' + \overline{t}t') - |r|^2\phi'$. The dwell time is derived directly from Eq. (11) and reads $\tau_d = \tau_g - \mathbf{Re}(re^{-i\phi})\phi'/\cos\phi$. From Eq. (18) we get

$$\tau_i = -\frac{\sin\phi}{|E|\cos^2\phi}\mathbf{Re}(re^{-i\phi}). \tag{20}$$

This expression is similar to that in Ref. 18 and satisfies $\tau_g = \tau_d + \tau_i$.

For a rectangular barrier with height V_0 and width L, the reflection amplitude r for the incident and reflected waves (19) can be written as[24]

$$r = -e^{i\phi}EV_0\sin\phi\sin(k_mL)/(k_mzv_F^2). \tag{21}$$

Here $k_m = \sqrt{(E-V_0)^2 - k_y^2}$ and $z = k_{in}\cos(k_mL) - i(k_{in}^2 - EV_0v_F^{-2})\sin(k_mL)/k_m$. Substituting Eq. (21) into (20), we yield

$$\tau_i = \frac{EV_0\sin^2\phi}{v_F^2|z|^2\cos\phi}\frac{\sin(k_mL)}{k_mv_F}\cos(k_mL). \tag{22}$$

We see that under the rectangular barrier τ_i is generally finite. It vanishes only at reflection zeros (where $\phi = 0$ or k_mL/π is integer) or in the case that k_mL/π is half-integer.

III. TUNNELING TIME OF ELECTRONS IN TOPOLOGICAL SURFACE STATES

We take helical electrons in topological surface states[25] as an example to examine numerically the effect of evanescent modes on the tunneling time. The considered topological insulator (Bi_2Te_3 or Bi_2Se_3) has only one gapless Dirac cone in its surface bands and can exhibit a hexagonal snowflake Fermi surface[26–29]. Near the Dirac point, the effective surface Hamiltonian including the trigonal warping term[26] and a rectangular barrier is written as

$$\hat{H} = v_F(\sigma_y\hat{k}_x - \sigma_x\hat{k}_y) + \lambda(\hat{k}_x^3 - 3\hat{k}_x\hat{k}_y^2)\sigma_z + V(\mathbf{r})\sigma_0. \tag{23}$$

Here the momentum $\hat{k}_y = -i\partial_y$ is along the Γ-M direction, λ is the warping parameter, and σ_0 is a unit matrix. For simplicity, the term $(\hat{k}_x^2 + \hat{k}_y^2)/2m$ is neglected. In the numerical calculation, the two material parameters for Bi_2Te_3 are taken as[26,27] $v_F = 255$ meV nm and $\lambda = 250$ meV nm^3.

The potential barrier has a width L and height V_0. Due to the anisotropy of the warping term, we consider two orientations of the applied barrier: (1) the x direction where $V = V(x)$ and the momentum $q = k_y$ is conserved; (2) the y direction where $V = V(y)$ and the momentum $q = k_x$ is

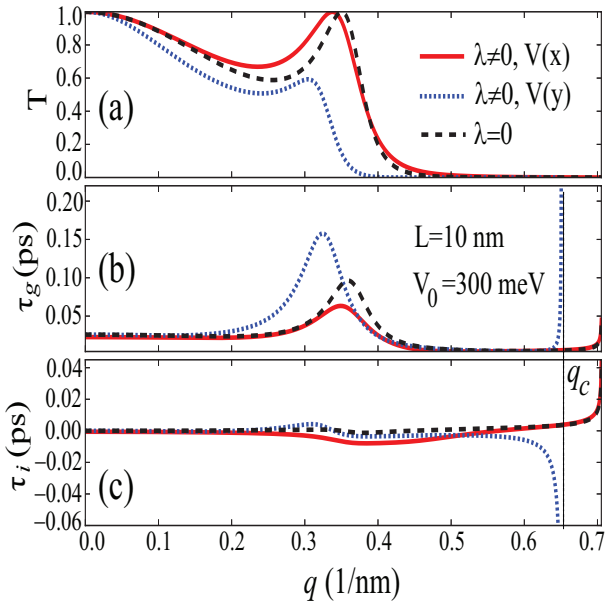

FIG. 2: (Color online) Transmission (a), group delay τ_g (b) and interference delay τ_i (c) plotted as a function of conserved momentum q, for helical electrons described by Eq. (23) in the single-mode transport regime. The red solid and blue dotted lines are for the barrier along the x and y direction. The results for the linear-in-momentum Hamiltonian ($\lambda = 0$) is presented as black dashed lines. The parameters are $E = 180$ meV, $V_0 = 300$ meV, and $L = 10$ nm.

a good quantum number. Here $V(x) = V_0\Theta(x)\Theta(L-x)$ with $\Theta(x)$ the Heaviside step function. For the two barrier orientations, an effective 1D Hamiltonian $\hat{H}(q)$ is obtained from Eq. (23) by the replacement $\hat{k}_y \to q$ or $\hat{k}_x \to q$. The scattering matrix method[30] is adopted to obtain the scattering states of $\hat{H}(q)$ and then the transmission probability T and the tunneling time. Note that one of the operator σ_x and σ_y transforms $\hat{H}(q)$ into $\hat{H}(-q)$. As a result, both the transmission probability and the tunneling time determined by $\hat{H}(q)$ are even functions of q. We calculate the dwell time directly from the definition Eq. (6) and indirectly from Eq. (16). Our numerical results confirm the agreement of the two methods.

For a small energy E such as $E = 180$ meV, the constant-energy surface in leads looks like a circle or hexagon[31]. For either the barrier $V(x)$ or $V(y)$, only a single ingoing mode can exist in leads. In Fig. 2, we plot the transmission T, the group delay τ_g, and the interference delay τ_i as a function of conserved momentum q. The barrier parameters are $V_0 = 300$ meV and $L = 10$ nm. In comparison with the results for the linear-in-momentum Hamiltonian ($\lambda = 0$), one can see that the warping term can enhance (suppress) the transmission and shorten (extend) the group delay as the transport is along the x (y) direction. For $\lambda = 0$, Eq. (23) is equivalent to the graphene Hamiltonian and thus the interference delay is given in Eq. (22). τ_i is noticeable only for $|q|$ near E/v_F due to the factor $\sin^2\phi/\cos\phi$. For the barrier $V(x)$ the warping term changes slightly the value of τ_i. In contrast, along the transport y direction τ_i can be altered drastically.

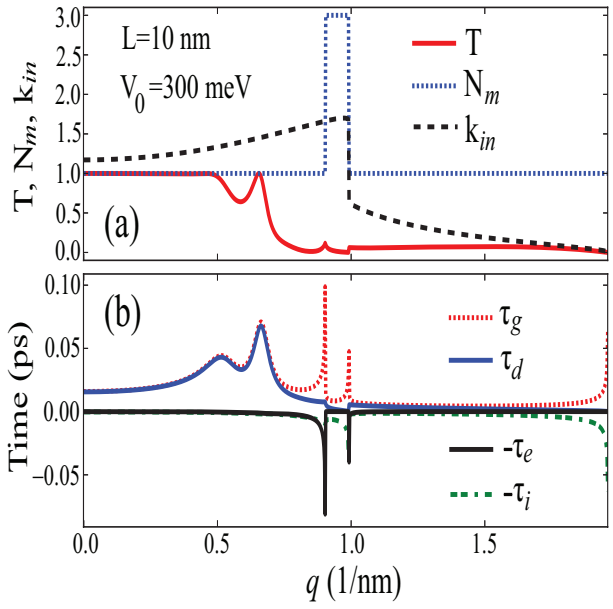

FIG. 3: (Color online) Transmission (a) and tunneling time (b) as a function of conserved momentum q for helical electrons described by Eq. (23) incident from the mode with the largest momentum k_{in}. The transport is along the x direction. The number of right-propagating modes N_m and k_{in} in the left lead are plotted in (a) for convenience. The parameters are $E = 500$ meV, $V_0 = 300$ meV, and $L = 10$ nm.

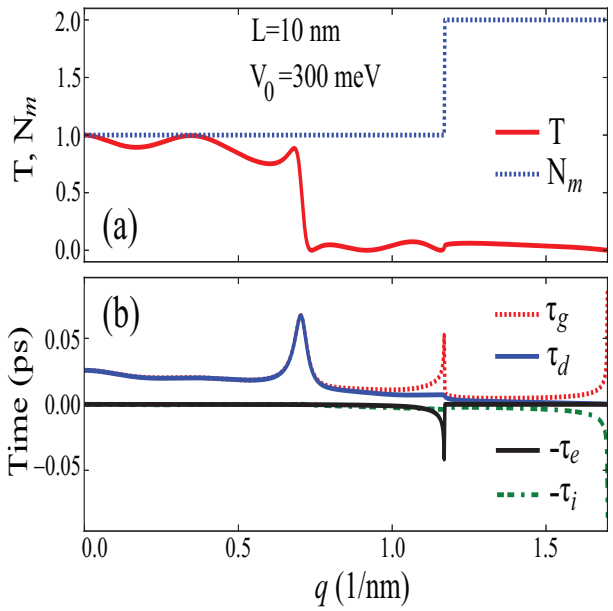

FIG. 4: (Color online) Same as Fig. 3 but for the potential barrier along the y direction.

When q is near the critical value q_c above which propagating modes disappear, τ_i can approach -0.35 ps while τ_g can be up to 0.36 ps. In the transmission-blocked regime, τ_d (not shown here) changes slightly. This observation indicates that $\tau_e = \tau_g - \tau_d - \tau_i$ is remarkable (up to 0.7 ps) for q near q_c.

When the incident energy meets $E > 1.45\sqrt{v_F^3/\lambda} \approx 373$ meV, the number of ingoing modes N_m in a lead can approach three (two) for the transport x (y) direction[31]. In Fig. 3 (Fig. 4) we take a high energy $E = 500$ meV to illustrate the features of tunneling time in the case of multichannel transport along the x (y) direction. The incident wave has the largest momentum k_{in} among ingoing modes in leads. In the region with $T > 0.5$ (and $N_m = 1$), the $\tau_d - q$ curve almost coincides with the $\tau_g - q$ curve. For q near E/v_F no transmission channel is open in the barrier region. Accordingly, the group delay goes up quickly which is mainly contributed by the interference delay. In the region with $N_m > 1$, no evanescent mode appears in leads and thus $\tau_e = 0$. More interesting features are seen near the onset of new ongoing modes. Here a sharp peak of the group delay forms, while the dwell time changes smoothly. Their difference is mainly caused by the evanescent waves. This can be understood qualitatively as follows. To remove the effect of evanescent waves in the left lead with decaying length L_d, one can extend the scattering boundary $x = 0$ to $x = -x_L < 0$ with $x_L \propto L_d$ which is equivalent to increase the original reflection phase by $k_{in}x_L$. Near the onset of a new ongoing mode, x_L increases quickly with the energy while k_{in} varies slowly. Therefore, these evanescent waves can contribute remarkably to τ_g. Another transition point of N_m is shown in Fig. 3(a), where a sudden drop occurs in the $k_{in} - q$ curve. This variation arises from the concave hexagrams in the snowflake equal-energy surface[26,31]. Near this transition, τ_d jumps with a small step while τ_g has a sharp peak. Their difference are caused both by the evanescent waves and interference delay.

IV. CONCLUSIONS AND REMARKS

In summary, for electron scattering states with many components we have derived a general relation between the Wigner group delay τ_g and Bohmian dwell time τ_d. Because the phase of scattering amplitudes is related to the spinor wave functions of corresponding propagating modes, it is necessary to redefine the group delay τ_g. The difference between τ_g and τ_d comes from both the interference delay and the evanescent modes. For electrons in topological surface states transporting through an electric barrier, we have examined the effect of trigonal warping on the tunneling time. The system with trigonal warping term can be in the multimode transport regime. It is found that near the onset of new modes, τ_g increases quickly and is contributed mainly by the evanescent modes.

For many quasi-1D systems like quantum waveguides with spin-orbit interaction[22] and quantum spin-Hall bars[23], we can represent their Hamiltonian in terms of a common set of orthogonal basis functions[30] and yield Eq. (1) after a proper truncation. The relation between τ_g and τ_d in our work can be used to study the tunneling time in these systems.

This work was supported by the NSF EPSCoR (Grant No. 1010094) and the National Natural Science Foundation of China (Grant No. 11174252).

Appendix A: Plane-wave solutions in a lead

In a lead with constant $\mathbf{A}_r$ $(0 \leq r \leq N)$, a plane-wave solution $\psi \exp(ikx)$ satisfies

$$[\mathbf{A}_0 - E\mathbf{I}_M]\psi + \sum_{r=1}^{N} k^r \mathbf{A}_r \psi = 0. \tag{A1}$$

Here $\mathbf{I}_M$ is the $M \times M$ unit matrix. Equation (A1) can be transformed into an equivalent eigen problem $\mathbf{B}X = kX$ with

$$\mathbf{B} = \begin{pmatrix} 0 & I_M & 0 & ... & 0 \\ 0 & 0 & I_M & ... & 0 \\ . & . & . & . & . \\ 0 & 0 & 0 & ... & I_M \\ B_{N1} & B_{N2} & B_{N3} & ... & B_{NN} \end{pmatrix}, \tag{A2}$$

$$X = \begin{pmatrix} \psi \\ k\psi \\ ... \\ k^{N-1}\psi \end{pmatrix}.$$

Here $\mathbf{B}_{N1} = -\mathbf{A}_N^{-1}(\mathbf{A}_0 - E\mathbf{I}_M)$, $\mathbf{B}_{Nr} = -\mathbf{A}_N^{-1}\mathbf{A}_{r-1} (r = 2, ..., N)$. The matrix $\mathbf{B}$ has NM eigen vectors X_1, X_2, ..., X_{NM} with corresponding eigen values k_1, k_2, ..., k_{NM}. The first M components of X_j comprise a vector ψ_j.

Appendix B: Probability current density in the considered one-dimensional systems

The time-dependent Schrödinger equation for the wave function Ψ and its Hermitian conjugate $\Psi^\dagger$ reads

$$\mathbf{A}_0\Psi + \sum_{r=1}^{N} \mathbf{A}_r \hat{k}_x^r \Psi = i\partial_t \Psi, \tag{B1}$$

$$\Psi^\dagger \mathbf{A}_0 + \sum_{r=1}^{N} (\hat{k}_x^r \Psi)^\dagger \mathbf{A}_r = -i\partial_t \Psi^\dagger. \tag{B2}$$

We multiply Eq. (B1) with $\Psi^\dagger$ from the left and multiply Eq. (B2) with Ψ from the right. After some algebra, one gets

$$\begin{aligned} i\partial_t(\Psi^\dagger\Psi) &= \sum_{r=1}^{N} [\Psi^\dagger \mathbf{A}_r (\hat{k}_x^r \Psi) - (\hat{k}_x^r \Psi)^\dagger \mathbf{A}_r \Psi] \\ &= \hat{k}_x J(\Psi, \Psi), \end{aligned} \tag{B3}$$

where $J(\Psi, \Psi)$ is the probability current density, and the function $J(\Psi_1, \Psi_2)$ is defined in Eq. (8) in the text.

The first property of J, Eq. (9) in the text, can be checked by using the identity

$$\begin{aligned} \hat{k}_x[(\hat{k}_x^s \Psi_1)^\dagger \mathbf{A}_r (\hat{k}_x^{r-1-s} \Psi_2)] &= (\hat{k}_x^s \Psi_1)^\dagger \mathbf{A}_r (\hat{k}_x^{r-s} \Psi_2) \\ &- (\hat{k}_x^{s+1} \Psi_1)^\dagger \mathbf{A}_r (\hat{k}_x^{r-1-s} \Psi_2). \end{aligned}$$

The second property of J, Eq. (10) in the text, is proved as

$$\begin{aligned} J(\Phi_1, \Phi_2) &= \sum_{r=1}^{N} \sum_{s=0}^{r-1} \bar{k}_1^s k_2^{r-1-s} \psi_1^\dagger \mathbf{A}_r \psi_2 \exp[i(k_2 - \bar{k}_1)x] \\ &= \exp[i(k_2 - \bar{k}_1)x] \sum_{r=1}^{N} \frac{k_2^r - \bar{k}_1^r}{k_2 - \bar{k}_1} \psi_1^\dagger \mathbf{A}_r \psi_2 \\ &= F \sum_{r=0}^{N} [\psi_1^\dagger (\mathbf{A}_r k_2^r \psi_2) - (\psi_1^\dagger \mathbf{A}_r \bar{k}_1^r)\psi_2] \\ &= F[\psi_1^\dagger (E_2 \psi_2) - (E_1 \psi_1^\dagger)\psi_2] \\ &= (E_2 - E_1) F \psi_1^\dagger \psi_2. \end{aligned}$$

Here the factor $F = \exp[i(k_2 - \bar{k}_1)x]/(k_2 - \bar{k}_1)$. In the third line we have used $\sum_{r=0}^{N} \mathbf{A}_r k_j^r \psi_j = E_j \psi_j$ for the mode $\Phi_j (j = 1, 2)$.

In the case $k_2 = \bar{k}_1$, $J(\Phi_1, \Phi_2)$ becomes

$$\sum_{r=1}^{N} r k_2^{r-1} \psi_1^\dagger \mathbf{A}_r \psi_2 = \Phi_1^\dagger (\hat{v} \Phi_2),$$

where the velocity operator

$$\hat{v} = \frac{\partial \hat{H}}{\partial \hat{k}_x} = \sum_{r=1}^{N} r \mathbf{A}_r \hat{k}_x^{r-1}.$$

Thus for a propagating mode $\Phi(x) = \psi \exp(ikx)$ in a lead, the mean velocity v_k equals $J(\Phi, \Phi)/(\Phi^\dagger \Phi)$.

For $N = 2$, one has

$$J(\Psi, \Psi) = i\partial_x \Psi^\dagger \mathbf{A}_2 \Psi - i\Psi^\dagger \mathbf{A}_2 \partial_x \Psi + \Psi^\dagger \mathbf{A}_1 \Psi.$$

In this case the probability current density $J(\Psi, \Psi)$ can be expressed as $\mathbf{Re}(\Psi^\dagger \hat{v} \Psi)$, Note that[32] when the relation $J(\Psi, \Psi) = \mathbf{Re}(\Psi^\dagger \hat{v} \Psi)$ holds for any state Ψ, one must have $N \leq 2$.

Appendix C: Expression of the generalized group delay τ_g

To calculate the limit of Q in Eq. (14), we expand all quantities of the state Ψ_2 up to the second order of ΔE,

$$f(E + \Delta E) = f(E) + f'(E)\Delta E + f''(E)\frac{(\Delta E)^2}{2} + ..., \tag{C1}$$

where the prime denotes the derivative with respect to the energy E. We get

$$\begin{aligned} Q &= \sum_{j\in LP} \bar{r}_j(r_j + r'_j\Delta E + ...)\frac{\psi_j^\dagger(\psi_j + \psi'_j\Delta E + ...)}{\Delta E(k'_j + ...)} \\ &+ \frac{\psi_{in}^\dagger(\psi_{in} + \psi'_{in}\Delta E + ...)}{\Delta E(k'_{in} + ...)} \\ &- \sum_{j\in RP} \bar{t}_j(t_j + t'_j\Delta E + ...)\frac{\psi_j^\dagger(\psi_j + \psi'_j\Delta E + ...)}{\Delta E(k'_j + ...)} \\ &= \sum_{j\in LP} \frac{|r_j|^2\psi_j^\dagger\psi_j}{\Delta E(k'_j + ...)} - \sum_{j\in RP} \frac{|t_j|^2\psi_j^\dagger\psi_j}{\Delta E(k'_j + ...)} \\ &+ \frac{\psi_{in}^\dagger\psi_{in}}{\Delta E(k'_{in} + ...)} + \sum_{j\in LP} \frac{\bar{r}_j\psi_j^\dagger(r_j\psi_j)'}{k'_j} \\ &- \sum_{j\in RP} \frac{\bar{t}_j\psi_j^\dagger(t_j\psi_j)'}{k'_j} + \frac{\psi_{in}^\dagger\psi'_{in}}{k'_{in}} + O(\Delta E). \end{aligned} \tag{C2}$$

The sum of the first three terms in the last equation is further calculated as

$$\begin{aligned} &\sum_{j\in LP} \frac{|r_j|^2\psi_j^+\psi_j(1 - \frac{k''_j}{2k'_j}\Delta E)}{\Delta E k'_j} + \frac{\psi_{in}^+\psi_{in}(1 - \frac{k''_{in}}{2k'_{in}}\Delta E)}{\Delta E k'_{in}} \\ &- \sum_{j\in RP} \frac{|t_j|^2\psi_j^+\psi_j(1 - \frac{k''_j}{2k'_j}\Delta E)}{\Delta E k'_j} + O(\Delta E) \\ &= \sum_{j\in LP} \frac{|r_j|^2 k''_j}{2k'_j} + \sum_{j\in RP} \frac{|t_j|^2 k''_j}{2k'_j} - \frac{k''_{in}}{2k'_{in}} + O(\Delta E). \end{aligned}$$

Here we have used $\sum_{j\in LP}|r_j|^2 + \sum_{j\in RP}|t_j|^2 = 1$ and the velocity normalization for propagating modes, $\psi_j^\dagger\psi_j = \pm k'_j(E)$. Replacing k'_j and k''_j with $\pm\psi_j^\dagger\psi_j$ and $\pm[(\psi_j^+)'\psi_j + \psi_j^+\psi'_j]$, we find the full expression of Q,

$$\begin{aligned} Q &= \sum_{j\in LP} [|r_j|^2\frac{(\psi_j^+)'\psi_j - \psi_j^+\psi'_j}{2\psi_j^\dagger\psi_j} - \bar{r}_j r'_j] \\ &+ \sum_{j\in RP} [|t_j|^2\frac{(\psi_j^+)'\psi_j - \psi_j^+\psi'_j}{2\psi_j^\dagger\psi_j} - \bar{t}_j t'_j] \\ &+ \frac{\psi_{in}^+\psi'_{in} - (\psi_{in}^+)'\psi_{in}}{2\psi_{in}^\dagger\psi_{in}} + O(\Delta E). \end{aligned} \tag{C3}$$

From Eqs. (C3) and (13) one can check that both $\lim_{\Delta E\to 0} Q$ and $\lim_{\Delta E\to 0} P$ are purely imaginary. After some algebra, we yield Eq. (15) in the text from Eq. (C3).

Appendix D: Probability current density of general one-dimensional systems

When the matrix $\mathbf{A}_r$ ($r \geq 1$) is position-dependent, the term $\mathbf{A}_r\hat{k}_x^r$ in Eq. (1) should be symmetrized to ensure the Hermiticity of the Hamiltonian $\hat{H}$. The symmetrized form of $\mathbf{A}_r\hat{k}_x^r$ is chosen as

$$\hat{H}_r \equiv \hat{k}_x^t\mathbf{A}_r\hat{k}_x^t \tag{D1}$$

if r is an even number $r = 2t$ and

$$\hat{H}_r \equiv (\hat{k}_x^t\mathbf{A}_r\hat{k}_x^{t-1} + \hat{k}_x^{t-1}\mathbf{A}_r\hat{k}_x^t)/2 \tag{D2}$$

when r is an odd number $r = 2t-1$, *which has the minimum requirement of the smoothness of* $\mathbf{A}_r(x)$ [$\hat{k}_x^{t-1}\mathbf{A}_r(x)$ *is piecewise continuous*].

There exists a bilinear function $J(\Psi_1, \Psi_2)$ satisfying

$$\Psi_1^\dagger(\hat{H}\Psi_2) - (\hat{H}\Psi_1)^\dagger\Psi_2 \equiv \hat{k}_x J(\Psi_1, \Psi_2). \tag{D3}$$

We write $J = J_1 + J_2 + ... + J_N$ where the probability current density J_r is due to the Hamiltonian $\hat{H}_r$ for $r = 1, 2, ..., N$. Equation (D3) holds when every $\hat{J}_r$ meets

$$\hat{k}_x J_r(\Psi_1, \Psi_2) = \Psi_1^\dagger(\hat{H}_r\Psi_2) - (\hat{H}_r\Psi_1)^\dagger\Psi_2. \tag{D4}$$

For an even number $r = 2t$, we find

$$\begin{aligned} J_r &= i\sum_{s=0}^{t-1}(-1)^{s+t}[\partial_x^s\Psi_1^\dagger\partial_x^{t-1-s}(\mathbf{A}_r\partial_x^t\Psi_2) \\ &- \partial_x^{t-1-s}(\partial_x^t\Psi_1^\dagger\mathbf{A}_r)\partial_x^s\Psi_2] \\ &= i\sum_{s,p\geq 0}(-1)^{s+t}C_{t-1-s}^p(\partial_x^s\Psi_1^\dagger\partial_x^p\mathbf{A}_r\partial_x^{r-1-s-p}\Psi_2 \\ &- \partial_x^{r-1-s-p}\Psi_1^\dagger\partial_x^p\mathbf{A}_r\partial_x^s\Psi_2). \end{aligned} \tag{D5}$$

We check Eq. (D4) by calculating $\mathbf{DJ} \equiv (-1)^t\hat{k}_x J_r$ as

$$\begin{aligned} \mathbf{DJ} &= \sum_{s,p\geq 0}(-1)^s C_{t-1-s}^p[\partial_x^{s+1}\Psi_1^\dagger\partial_x^p\mathbf{A}_r\partial_x^{r-1-s-p}\Psi_2 \\ &- \partial_x^{r-1-s-p}\Psi_1^\dagger\partial_x^p\mathbf{A}_r\partial_x^{s+1}\Psi_2] \\ &+ \sum_{s,p\geq 0}(-1)^s C_{t-1-s}^p[\partial_x^s\Psi_1^\dagger\partial_x^{p+1}\mathbf{A}_r\partial_x^{r-s-p-1}\Psi_2 \\ &- \partial_x^{r-1-s-p}\Psi_1^\dagger\partial_x^{p+1}\mathbf{A}_r\partial_x^s\Psi_2] \\ &+ \sum_{s,p\geq 0}(-1)^s C_{t-1-s}^p[\partial_x^s\Psi_1^\dagger\partial_x^p\mathbf{A}_r\partial_x^{r-s-p}\Psi_2 \\ &- \partial_x^{r-s-p}\Psi_1^\dagger\partial_x^p\mathbf{A}_r\partial_x^s\Psi_2]. \end{aligned} \tag{D6}$$

The first line of Eq. (D6) after substituting $s+1 \to s$ becomes

$$\begin{aligned} &\sum_{p\geq 0, s\geq 1}(-1)^{s-1}C_{t-s}^p[\partial_x^s\Psi_1^\dagger\partial_x^p\mathbf{A}_r\partial_x^{r-s-p}\Psi_2 \\ &-\partial_x^{r-s-p}\Psi_1^\dagger\partial_x^p\mathbf{A}_r\partial_x^s\Psi_2]. \end{aligned} \tag{D7}$$

The second line of Eq. (D6) after substituting $p+1 \to p$ turns to

$$\begin{aligned} &\sum_{s,p\geq 0}(-1)^s C_{t-1-s}^{p-1}[\partial_x^s\Psi_1^\dagger\partial_x^p\mathbf{A}_r\partial_x^{r-s-p}\Psi_2 \\ &-\partial_x^{r-s-p}\Psi_1^\dagger\partial_x^p\mathbf{A}_r\partial_x^s\Psi_2]. \end{aligned} \tag{D8}$$

After these procedures, we get

$$\begin{aligned}\mathbf{DJ} &= \sum_{s,p\geq 0}(-1)^s[C^p_{t-1-s}-C^p_{t-s}+C^{p-1}_{t-1-s}]\\ &\quad \partial_x^s\Psi_1^\dagger\partial_x^p\mathbf{A}_r\partial_x^{r-s-p}\Psi_2\\ &+ \sum_{s,p\geq 0}(-1)^s[-C^p_{t-1-s}+C^p_{t-s}-C^{p-1}_{t-1-s}]\\ &\quad \partial_x^{r-s-p}\Psi_1^\dagger\partial_x^p\mathbf{A}_r\partial_x^s\Psi_2\\ &+ \sum_{p\geq 0}C^p_t[\Psi_1^\dagger\partial_x^p\mathbf{A}_r\partial_x^{r-p}\Psi_2-\partial_x^{r-p}\Psi_1^\dagger\partial_x^p\mathbf{A}_r\Psi_2]\end{aligned}$$

The first and second lines of this equation vanish due to

$$C^p_{t-s}=C^p_{t-1-s}+C^{p-1}_{t-1-s}. \tag{D9}$$

Comparing the last expression of $\mathbf{DJ}$ with

$$\begin{aligned}&\Psi_1^\dagger(\hat{k}_x^t\mathbf{A}_r\hat{k}_x^t\Psi_2)-(\hat{k}_x^t\mathbf{A}_r\hat{k}_x^t\Psi_1)^\dagger\Psi_2\\ &= (-1)^t\sum_{p\geq 0}C^p_t[\Psi_1^\dagger\partial_x^p\mathbf{A}_r\partial_x^{r-p}\Psi_2-\partial_x^{r-p}\Psi_1^\dagger\partial_x^p\mathbf{A}_r\Psi_2],\end{aligned}$$

we get $\hat{k}_xJ_{2t}=\Psi_1^\dagger(\hat{k}_x^t\mathbf{A}_r\hat{k}_x^t\Psi_2)-(\hat{k}_x^t\mathbf{A}_r\hat{k}_x^t\Psi_1)^\dagger\Psi_2$.

For an odd number $r=2t-1$, We can take $\mathbf{I}\equiv 2J_r(-1)^{t-1}$ as

$$\begin{aligned}\mathbf{I} &= \sum_{p=1}^{2}\sum_{s=0}^{t-p}(-1)^s[\partial_x^s\Psi_1^\dagger\partial_x^{t-p-s}(\mathbf{A}_r\partial_x^{t+p-2}\Psi_2)\\ &\quad +\partial_x^{t-p-s}(\partial_x^{t+p-2}\Psi_1^\dagger\mathbf{A}_r)(\partial_x^s\Psi_2)]\\ &= \sum_{s,p,q}(-1)^sC^q_{t-p-s}[\partial_x^s\Psi_1^\dagger\partial_x^q\mathbf{A}_r\partial_x^{2t-2-s-q}\Psi_2\\ &\quad +\partial_x^{2t-2-s-q}\Psi_1^\dagger\partial_x^q\mathbf{A}_r\partial_x^s\Psi_2].\end{aligned} \tag{D10}$$

Then we get $\mathbf{DI}\equiv\partial_x\mathbf{I}=T_1+T_2+T_3$ with

$$\begin{aligned}T_1 &= \sum_{s,p,q}(-1)^sC^q_{t-p-s}[\partial_x^{s+1}\Psi_1^\dagger\partial_x^q\mathbf{A}_r\partial_x^{2t-2-s-q}\Psi_2\\ &\quad +\partial_x^{2t-2-s-q}\Psi_1^\dagger\partial_x^q\mathbf{A}_r\partial_x^{s+1}\Psi_2]\\ &= \sum_{p,q,s\geq 1}(-1)^{s-1}C^q_{t-p-s+1}[\partial_x^s\Psi_1^\dagger\partial_x^q\mathbf{A}_r\partial_x^{r-s-q}\Psi_2\\ &\quad +\partial_x^{r-s-q}\Psi_1^\dagger\partial_x^q\mathbf{A}_r\partial_x^s\Psi_2],\end{aligned}$$

$$\begin{aligned}T_2 &= \sum_{s,p,q}(-1)^sC^q_{t-p-s}[\partial_x^s\Psi_1^\dagger\partial_x^q\mathbf{A}_r\partial_x^{r-s-q}\Psi_2\\ &\quad +\partial_x^{r-s-q}\Psi_1^\dagger\partial_x^q\mathbf{A}_r\partial_x^s\Psi_2],\end{aligned}$$

$$\begin{aligned}T_3 &= \sum_{s,p,q}(-1)^sC^q_{t-p-s}[\partial_x^s\Psi_1^\dagger\partial_x^{q+1}\mathbf{A}_r\partial_x^{2t-2-s-q}\Psi_2\\ &\quad +\partial_x^{2t-2-s-q}\Psi_1^\dagger\partial_x^{q+1}\mathbf{A}_r\partial_x^s\Psi_2]\\ &= \sum_{s,p,q}(-1)^sC^{q-1}_{t-p-s}[\partial_x^s\Psi_1^\dagger\partial_x^q\mathbf{A}_r\partial_x^{r-s-q}\Psi_2\\ &\quad +\partial_x^{r-s-q}\Psi_1^\dagger\partial_x^q\mathbf{A}_r\partial_x^s\Psi_2].\end{aligned}$$

Repeating the same procedure as before, we yield

$$\begin{aligned}\mathbf{DI} &= \sum_{s,p,q}(-1)^s[C^q_{t-p-s}-C^q_{t-p-s+1}+C^{q-1}_{t-p-s}]\\ &\quad \times\ (\partial_x^s\Psi_1^\dagger\partial_x^q\mathbf{A}_r\partial_x^{r-s-q}\Psi_2+\partial_x^{r-s-q}\Psi_1^\dagger\partial_x^q\mathbf{A}_r\partial_x^s\Psi_2)\\ &+ \sum_{p,q}C^q_{t-p+1}[\Psi_1^\dagger\partial_x^q\mathbf{A}_r\partial_x^{r-q}\Psi_2+\partial_x^{r-q}\Psi_1^\dagger\partial_x^q\mathbf{A}_r\Psi_2],\end{aligned}$$

where the first term vanishes due to Eq. (D9). The right-hand side of Eq. (D4) for $r=2t-1$ is expanded as

$$\begin{aligned}\Psi_1^\dagger(\hat{H}_r\Psi_2) &- (\hat{H}_r\Psi_1)^\dagger\Psi_2=\frac{(-i)^r}{2}\sum_{p,q}C^q_{t-p+1}\\ &\times\ (\Psi_1^\dagger\partial_x^q\mathbf{A}_r\partial_x^{r-q}\Psi_2+\partial_x^{r-q}\Psi_1^\dagger\partial_x^q\mathbf{A}_r\Psi_2),\end{aligned}$$

which together with the last expression of $\mathbf{DI}$ gives Eq. (D4).

From Eq. (D3) we know that the probability current density for a given state Ψ is $J(\Psi,\Psi)=\sum_{r=1}^N J^{(r)}$ with $J^{(r)}=J_r(\Psi,\Psi)$. From Eqs. (D5) and Eq. (D10) one gets

$$\begin{aligned}J^{(2t)} &= 2\mathbf{Re}\sum_{s=0}^{t-1}(\hat{k}_x^s\Psi)^\dagger\hat{k}_x^{t-1-s}(\mathbf{A}_{2t}\hat{k}_x^t\Psi),\\ J^{(2t-1)} &= \mathbf{Re}[\sum_{s=0}^{t-1}(\hat{k}_x^s\Psi)^\dagger\hat{k}_x^{t-1-s}(\mathbf{A}_{2t-1}\hat{k}_x^{t-1}\Psi)\\ &\quad +\sum_{s=0}^{t-2}(\hat{k}_x^s\Psi)^\dagger\hat{k}_x^{t-2-s}(\mathbf{A}_{2t-1}\hat{k}_x^t\Psi)].\end{aligned}$$

[1] L. A. MacColl, Phys. Rev. 40, 621 (1932).
[2] E. P. Wigner, Phys. Rev. **98**, 145 (1955).
[3] F. T. Smith, Phys. Rev. **118**, 349 (1960).
[4] E. H. Hauge and J. A. Steng, Rev. Mod. Phys. **61**, 917 (1989).
[5] R. Landauer and Th. Martin, Rev. Mod. Phys. **66**, 217 (1994).
[6] H. G. Winful, Phys. Rev. Lett. **91**, 260401 (2003).
[7] N. Yamada, Phys. Rev. Lett. **93**, 170401 (2004).
[8] P. Eckle, A. N. Pfeiffer, C. Cirelli, A. Staudte, R. Drner, H. G. Muller, M. Bttiker, and U. Keller, Science **322**, 1525 (2008).
[9] E. A. Galapon, Phys. Rev. Lett. **108**, 170402 (2012).
[10] A. S. Landsman and U. Keller, Phys. Rep. **547**, 1 (2015).
[11] R. Pazourek, S. Nagele, and J. Burgdoerfer, Rev. Mod. Phys. **87**, 765 (2015).
[12] T. Zimmermann, S. Mishra, B. R. Doran, D. F. Gordon, and A. S. Landsman, Phys. Rev. Lett. **116**, 233603 (2016).
[13] Z. H. Wu, K. Chang, J. T. Liu, X. J. Li, and K. S. Chan, J. Appl. Phys. **105**, 043702 (2009).
[14] Y. Y. Gong and Y. Guo, J. Appl. Phys. **106**, 064317 (2009).
[15] D. Dragoman and M. Dragoman, J. Appl. Phys. **107**, 054306 (2010).
[16] Z. J. Li, H. Zhao, Y. H. Nie, and J. Q. Liang, J. Appl. Phys. **113**, 043714 (2013).

[17] Y. Ban, L.J Wang, and X. Chen, J. Appl. Phys. **117**, 164307 (2015).
[18] Y. Song and H. C. Wu, J. Phys.: Condens. Matter **25**, 355301 (2013).
[19] C. S. Park, Phys. Rev. B **89**, 115423 (2014).
[20] E. Prada, P. San-Jose, and R. Aguado, Phys. Rev. B **86**, 180503(R) (2012).
[21] D. Rainis, L. Trifunovic, J. Klinovaja, and D. Loss, Phys. Rev. B **87**, 024515 (2013).
[22] L. B. Zhang, P. Brusheim, and H. Q. Xu, Phys. Rev. B **72**, 045347 (2005); D. Sánchez and L. Serra, Phys. Rev. B **74**, 153313 (2006).
[23] L. B. Zhang, F. Cheng, F. Zhai, and K. Chang, Phys.Rev. B **83**, 081402(R) (2011).
[24] F. Zhai, Nanoscale **4**, 6527 (2012).
[25] X. L. Qi and S. C. Zhang, Rev. Mod. Phys. **83**, 1057 (2011).
[26] Liang Fu, Phys. Rev. Lett. **103**, 266801 (2009).
[27] Y. L. Chen, J. G. Analytis, J.-H. Chu, Z. K. Liu, S.-K.Mo, X. L. Qi, H. J. Zhang, D. H. Lu, X. Dai, Z. Fang, S. C. Zhang, I. R. Fisher, Z. Hussain, and Z.-X. Shen, Science **325**, 178 (2009).
[28] Z. Alpichshev, J. G. Analytis, J.-H. Chu, I. R. Fisher, Y. L. Chen, Z. X. Shen, A. Fang, and A. Kapitulnik, Phys. Rev. Lett. **104**, 016401 (2010).
[29] K. Kuroda, M. Arita, K. Miyamoto, M. Ye, J. Jiang, A. Kimura, E. E. Krasovskii, E. V. Chulkov, H. Iwasawa, T. Okuda, K. Shimada, Y. Ueda, H. Namatame, and M. Taniguchi, Phys. Rev. Lett. **105**, 076802 (2010).
[30] H. Xu, Phys. Rev. B **50**, 8469 (1994); ibid. **52**, 5803 (1995); L. B. Zhang, F. Zhai, and H. Q. Xu, Phys. Rev. B **74**, 195332 (2006).
[31] J. An and C. S. Ting, Phys. Rev. B **86**, 165313 (2012).
[32] Y. Li and R. B. Tao, Phys. Rev. B **75**, 075319 (2007).